Editors' Suggestion | Featured in Physics

All-Optical Synchronization of Remote Optomechanical Systems

Jin Li,* Zhong-Hao Zhou,* Shuai Wan,* Yan-Lei Zhang, Zhen Shen, Ming Li,†
Chang-Ling Zou, Guang-Can Guo, and Chun-Hua Dong‡

CAS Key Laboratory of Quantum Information, University of Science and Technology of China, Hefei 230026, People's Republic of China
and CAS Center For Excellence in Quantum Information and Quantum Physics, University of Science and Technology of China, Hefei, Anhui 230026, People's Republic of China

(Received 22 March 2022; accepted 14 June 2022; published 5 August 2022)

Synchronization and frequency locking between remote mechanical oscillators are of scientific and technological importance. The key challenges are to align the oscillation frequencies and realize strong nonlinear interaction of both oscillators to a common carrier capable of long-distance transmission. Here, we experimentally realize the all-optical synchronization between two different optomechanical systems, a microsphere and a microdisk. The mechanical oscillation of the microsphere induced by the radiation pressure is loaded onto the pump laser via the optomechanical interaction, which is directly transmitted through a 5-km-long single-mode fiber to excite the mechanical oscillation of the microdisk. By finely tuning both the optical and mechanical frequencies of the two microresonators, the oscillation of the microdisk is injection locked to the microsphere, resulting in a synchronized phase relation of the two systems. Our results push a step forward the long-distance synchronization network using optomechanical microresonators.

DOI: 10.1103/PhysRevLett.129.063605

Introduction.—Synchronization of different oscillators is a ubiquitous phenomenon in nature and has been widely studied for potential applications in revolutionized timing technologies, signal processing and microwave communication [1–6]. The nano- and micromechanical oscillators can interact at the micron scale via an electronic coupling or a physical connection to realize the synchronization [7–14]. The optomechanical systems, driven by the radiation pressure, are good candidates due to the high oscillation frequency, miniaturized size, and low-power threshold [15–20] for the long-distance all-optical synchronization [21]. However, many all-optical synchronizations have been observed in linearly coupled or dissipatively coupled microresonator arrays on the integrated chip [22–25], yet the oscillators are separated by only the order of micrometers, which has limited applications in synchronization networks.

Despite the natural advantage of an optomechanical system that links mechanical oscillators to photons, experimental realization of the synchronization of remote optomechanical systems is challenging. First, due to the optical and mechanical dispersion and the unavoidable statistical variations in fabrication processes, it is difficult to simultaneously align both the optical and mechanical modes in different systems, especially for oscillators with different structures and materials. Things even get worse as detrimental thermal and nonlinear effects arise under operation by lasers [25–29]. Second, the amplitude of the mechanical oscillation decays during the transmission with inevitable optical loss, which limits the distance of synchronization. The master-slave locking scheme for separated optomechanical oscillators has been put forward by converting the light to rf signals and reloading the mechanical oscillation to the laser via the electro-optic modulators [30], during which the mechanical oscillation amplitude can be amplified to compensate the optical loss. However, the incoherent detection process destroys the phases of the oscillations and also is difficult for high-frequency oscillators.

In this Letter, we demonstrate the all-optical synchronization between a microdisk and a microsphere separated 5 km apart with a single coherent laser. Because of the thermal-optic and optical spring effect [31,32], we overcome the challenges in the simultaneous alignment of both the optical and mechanical modes in different optomechanical systems. Then, a coherent laser is used to drive the microsphere above the self-oscillation threshold, and the generated sideband tone together with the residue pump are guided to the microdisk through a 5-km-long fiber for injection locking to the microsphere. The phase locking is characterized by the power spectral density of the output fields and the trajectories in the phase space for both oscillators. Our work holds the promise of constructing long-distance synchronization networks of optomechanical systems.

Principle of synchronization.—Figure 1(a) illustrates two cascaded microresonators with small mechanical and optical frequency mismatches connected by an optical fiber. The optomechanical interaction of the two systems [21] both follow the Hamiltonian ($\hbar = 1$)

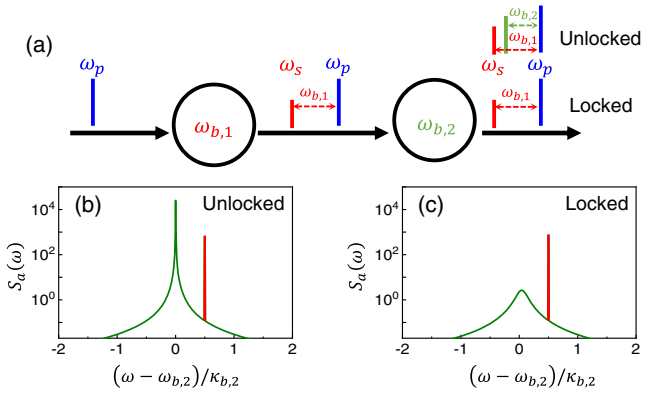

FIG. 1. All-optical synchronization by optomechanical injection locking. (a) Illustration of two cascaded optomechanical systems driven by a monochromatic laser. The sideband generated by the first system serves as the seed for the injection locking of the second system. For simplicity, only the strongest sideband generated by the optomechanical interaction is illustrated. (b),(c) Typical power spectral density of the second cavity at unlocked and locked states, respectively.

$$H = \omega_{a,i} a_i^\dagger a_i + \omega_{b,i} b_i^\dagger b_i + \hbar g_i a_i^\dagger a_i (b_i + b_i^\dagger), \quad (1)$$

where $i \in \{1, 2\}$ represents the first and second optomechanical resonators, respectively. $a^\dagger(b^\dagger)$ and $a(b)$ are the optical (mechanical) creation and annihilation operators of the corresponding microresonator. $\omega_{a,i}$ and $\omega_{b,i}$ are the frequencies of the corresponding optical and mechanical modes, and g is the vacuum optomechanical coupling rate. Because of the causality, the second resonator does not influence the first resonator for negligible backscattering. Therefore, a single mechanical system can be solved independently following the common approaches in previous works [15] except for different inputs. Under blue-detuned drive on the optical mode, the effective interaction Hamiltonian in both mechanical systems reduces to (see the Supplemental Material [33])

$$H_{\text{eff}} = \Delta_a a^\dagger a + \omega_b b^\dagger b + (g_{\text{eff}} a^\dagger b^\dagger + g_{\text{eff}}^* a b), \quad (2)$$

where we have neglected the subscript i, and $\Delta_a = \omega_a - \omega_p$ is the frequency detuning with ω_p being the frequency of the pump field, $g_{\text{eff}} = g\alpha$, with α being the amplitude of the optical mode normalized in photon number. It describes the parametric photon-phonon pair generation process, which is similar to the widely studied optical parametric oscillation. This process takes place spontaneously due to the vacuum and thermal noises in both the optical and mechanical modes, which we refer to as PE in the following. Above the phonon-lasing threshold, the intracavity photon number of the pump laser is clamped to α_{th} while a sideband tone is generated, leading to the oscillation of the mechanical oscillator. The frequency of the sideband tone $\omega_s \approx \omega_p - \omega_{b,1}$ depends on not only the mechanical frequency of the microsphere but also the frequency and strength of the pump field.

Through the optical fiber, the residual pump and generated sideband with the frequency of ω_p and ω_s are injected into the second resonator. Similarly, the pump laser also drives the parametric interaction in Eq. (2). What is different, in addition to the PE process, is that the sideband generated by the first system also stimulates the photon-phonon pair generation process (SE). The SE process generates mechanical phonons with frequency exactly equal to that of the first oscillator, contrary to the broadband spectrum by noise-induced PE. The stronger the sideband amplitude, the higher the stimulated photon numbers. The two processes both consume the pump photons and thus compete with each other.

To see this process more explicitly, the power spectrum of the optical field inside the second cavity (except the pump) is derived as (see Supplemental Material for details [33])

$$\begin{aligned} S_a(\omega) &= \langle a^\dagger(\omega) a(\omega) \rangle \\ &= \frac{2\kappa_{a,1} |\xi_b^-|^2 \varepsilon_s^2}{|\xi_a^+ \xi_b^- - g^2 |\alpha|^2|^2} \delta(\Delta_s - \omega) \\ &\quad + \frac{1}{2\pi} \frac{2\kappa_b g^2 |\alpha|^2 (n_{\text{th}} + 1)}{|\xi_a^+ \xi_b^- - g^2 |\alpha|^2|^2}, \end{aligned} \quad (3)$$

where $\Delta_s = \omega_s - \omega_p$ is the relative detuning between the two frequency components in the output of the microsphere, $\xi_a^\pm = \mp i(\omega_a - \omega_p \mp \omega) - \kappa_a$, $\xi_b^\pm = \mp i(\omega_b \mp \omega) - \kappa_b$, and ε_s is proportional to the amplitude of the sideband from the first cavity. The first term represents the contribution of the SE process and only has a nonvanishing value when the frequency equals the input ω_s. The broadband spectrum in the second term is attributed to the PE process, which becomes narrow with the increase of the intracavity amplitude α. The two processes compete with each other through the backaction to the intracavity amplitude α of the pump field by the parametric interaction in Eq. (2). The presence of ε_s modifies α in the denominator of Eq. (3) and the efficiency of PE is suppressed. For weak ε_s, the modification is small, the PE is still significant, and one obtains the unlocked state [Fig. 1(b)]. Whereas for large sideband amplitude ε_s and small frequency difference between the sideband and $\omega_{b,2}$, the backaction from SE to α strongly suppresses the PE, and SE dominates the parametric process [Fig. 1(c)], manifesting the mechanism of injection locking [34].

Experimental verification.—The experiment setup is illustrated in Fig. 2. With a tapered fiber, the pump laser around 1558 nm was coupled into the microsphere to excite the mechanical oscillation. Because of the optomechanical interaction, the out-coupled light was modulated by the mechanical vibration. Then a beam splitter was used to extract 1% portion of the light to the detector PD1 for the characterization of the optical and mechanical modes of the microsphere, and the remaining 99% portion was guided

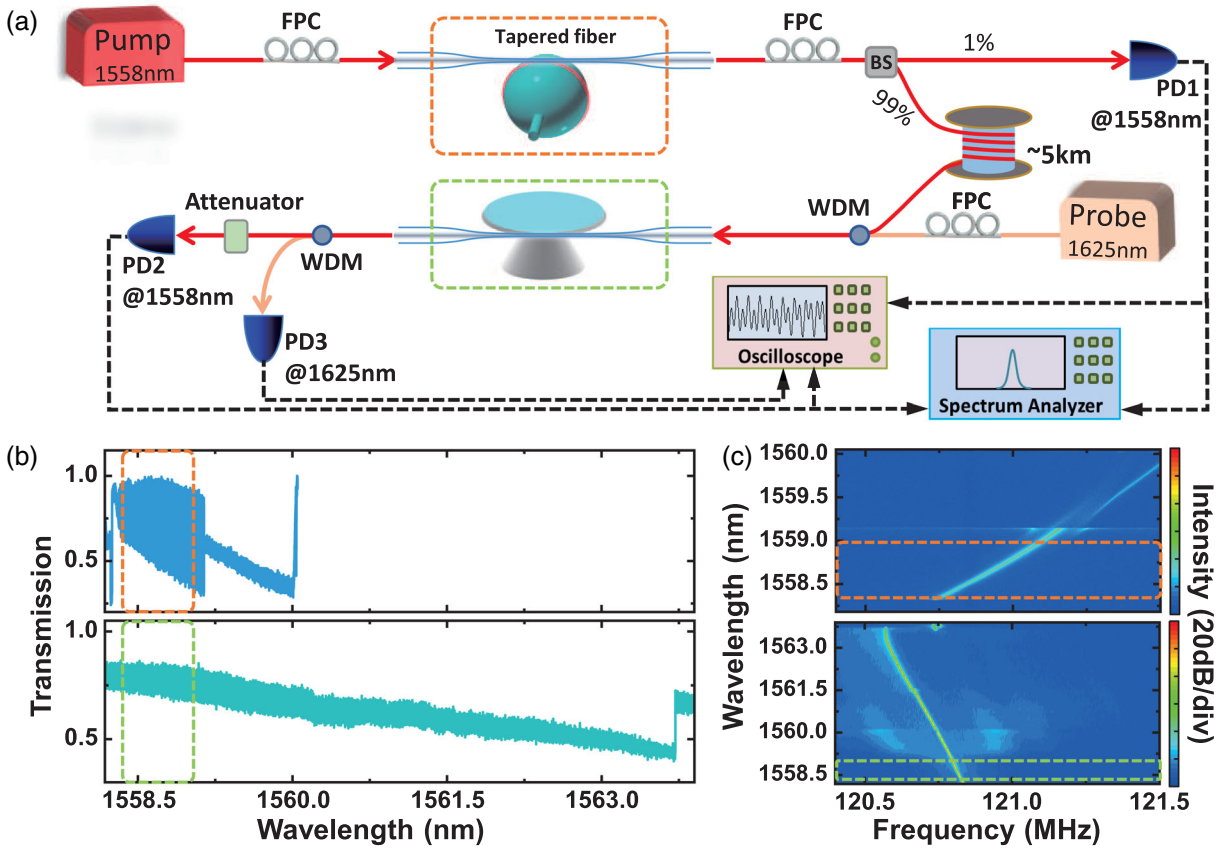

FIG. 2. (a) Schematic of the long-distance optomechanical synchronization setup. Two different kinds of optomechanical systems are driven through the pump laser around 1558 nm. A probe laser around 1625 nm is used to detect the mechanical vibration of the microdisk and confirm the realization of synchronization. FPC, fiber polarization controller; PD, photodetector; WDM, wavelength-division multiplexing. (b) The typical transmissions of the optical modes under thermal-optic and optomechanical effects, when the pump laser is scanning through the resonances of microsphere (upper) and the microdisk (bottom) individually. (c) The relevant mechanical frequency during the scanning process of (b). The boxes show the appropriate optical and mechanical frequencies for the synchronization.

through a standard single-mode fiber (12 m or 5 km) and coupled into the second microresonator, e.g., an on-chip microdisk, through another tapered fiber. The output field from the microdisk was then guided to the detector PD2 after attenuation. All experiments were performed at room temperature, and both optomechanical systems were placed in the cleaning chambers to reduce the interference of the contaminants and the perturbation of air.

The silica microsphere with a diameter of 38.7 μm was fabricated using a CO_2 laser. The loaded Q factor of the pumped optical mode is 3.56×10^7, while the mechanical frequency is $\omega_{b,1}/2\pi \approx 120.49$ MHz, with a damping rate of $\kappa_{b,1}/2\pi \approx 110.4$ kHz. The silicon microdisk with a radius of 20.88 μm was chosen to match the mechanical frequency of the microsphere. The loaded Q factor of the pumped mode is 5.12×10^4, and the mechanical frequency is $\omega_{b,2}/2\pi \approx 120.90$ MHz, which is only slightly deviated from $\omega_{b,1}$ for the synchronization. The damping rate of the mechanical resonance is $\kappa_{b,2}/2\pi \approx 30.9$ kHz. In addition, for the all-optical synchronization of different optomechanical systems, the resonant frequencies of optical modes in both optomechanical systems should be also tuned to match each other for the simultaneous near-resonant excitation on both cavities from the pump laser [35]. By scanning the pump laser through the optical modes, we obtained an appropriate region of two microresonators to match these requirements due to the thermal-optic effect [36], as shown in the dot boxes of Fig. 2(b) (see Supplemental Material [33]). The corresponding mechanical frequency variations are depicted in Fig. 2(c). Because of the optical spring effect of the mechanical vibrations [31,32], the mechanical frequencies of these microresonators change with different directions when the pump laser is scanning through the microresonators because of the different coupling regimes [31,32]. In the range of the red and the green regions in Figs. 2(b) and 2(c), the mechanical frequency difference could be tuned inside the injection locking range; therefore, two microresonators could vibrate at the same frequency with a fixed phase relation [21].

Figure 3(a) shows the dynamic evolution of the power spectrum detected by PD2 as the pump laser simultaneously coupled into the microresonators and scanning from 1558.822 to 1558.922 nm when two optomechanical systems separated with the single-mode fiber of 12 m. Because of the loss of optical elements, the power of the laser field decreases from 33.3 mW at the microsphere to 18.57 mW (∼2.5 dB) at the microdisk, which is still strong enough for the phonon-lasing threshold. At the beginning, the lasing frequency difference between the two resonators is too large so that the down-converted light from the microsphere cannot suppress the noise-induced spontaneous emission in the microdisk, and we observed multiple peaks in the detector PD2. In this regime, there is no fixed phase relation between the phonon lasers, since the two resonators experience independent vacuum and thermal noises. By further reducing the lasing frequency difference, the SE successfully suppresses the PE and the power spectrum of the output field reduces to a single peak, demonstrating that two resonators vibrate at a synchronized

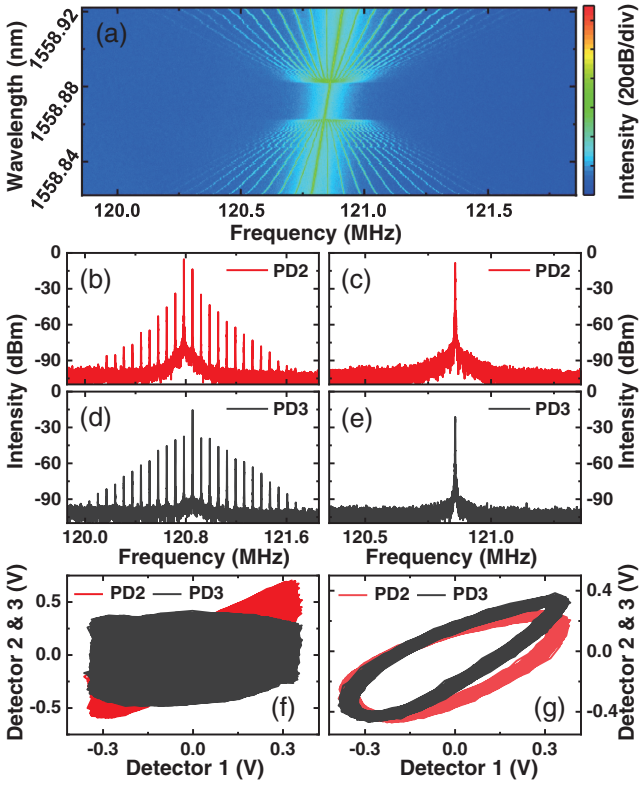

FIG. 3. Experimental results show the synchronization of the two optomechanical systems separated with the single-mode fiber of 12 m. (a) The dynamic evolution of the power spectrum detected by PD2 as the pump laser simultaneously coupled into the microresonators. (b),(c) The typical power spectral density with the pump laser of the nonsynchronization and synchronization states by PD2. (d),(e) The typical power spectral density with the probe laser of the nonsynchronization and synchronization states by PD3. (f),(g) Phase portraits of the optomechanical oscillations (f) before and (g) after synchronization.

frequency [Fig. 3(a)]. In addition, it should be pointed out that the synchronization has taken place when the mechanical frequencies close enough due to the optical spring effect, which also breaks the requirement because of the opposite shifting. Finally, as shown in the upper region of Fig. 3(a), the system can go out of the injection locking range and lose the synchronization state with further increase of the pump wavelength.

Figures 3(b) and 3(c) show the typical power spectral densities (PSDs) of the nonsynchronization and synchronization states from Fig. 3(a). In the nonsynchronized case, two sidebands with different frequencies can be generated by the two optomechanical interactions (Fig. 1), which further mix with each other by the four-wave mixing in the resonator and leads to a comblike output field with multiple frequency components [Fig. 3(b)]. When two mechanical systems are synchronized, the spectrum shows only one remarkable mechanical vibration frequency, i.e., the mechanical vibration frequency of the microsphere, and the noise background of spontaneous emission from the microdisk is orders of magnitude weaker. This electronic spectrum agrees pretty well with the optical spectrum in Fig. 1(c), demonstrating the response of the microdisk is injection locked to the microsphere.

It should be noted that each microresonator contains plenty of resonant modes, which all interact with the same mechanical mode. Once the microdisk is synchronized to the microsphere, any probe fields on the modes of the microdisk will be modulated by the mechanical vibration. To further confirm the process of the synchronization, we probe the microdisk with a laser around 1625 nm and measure the optical field at PD3, which is enabled by two wavelength-division multiplexers (1550/1620 nm). Figures 3(d) and 3(e) show the PSD signals from PD3, corresponding to the nonsynchronization and synchronization states, respectively. Since the 1550 and 1625 nm optical modes interact with each other by cross-phase-modulation, the multifrequency components' oscillation in the 1550 nm band can be transferred to 1625 nm, generating the multiple peaks in Fig. 3(d). These results unambiguously demonstrate that the mechanical oscillation of the microdisk was actually injection locked to the microsphere.

To get insight into the dynamical behavior of the synchronization, we directly measured the phase locking of the optomechanical systems by simultaneously tracking the trajectory of three detectors with a four-channel oscilloscope. As shown in Figs. 3(f) and 3(g), the phases of two microresonators can be extracted independently from the signals of PD1, PD2, and PD3, respectively. In the nonsynchronization case, the phase portraits cover a full rectangle as shown in Fig. 3(f) due to the strong PE in the microdisk. With properly reduced detuning, the optomechanical interaction is dominated by the SE induced by the seeding photons from the microsphere. The regular

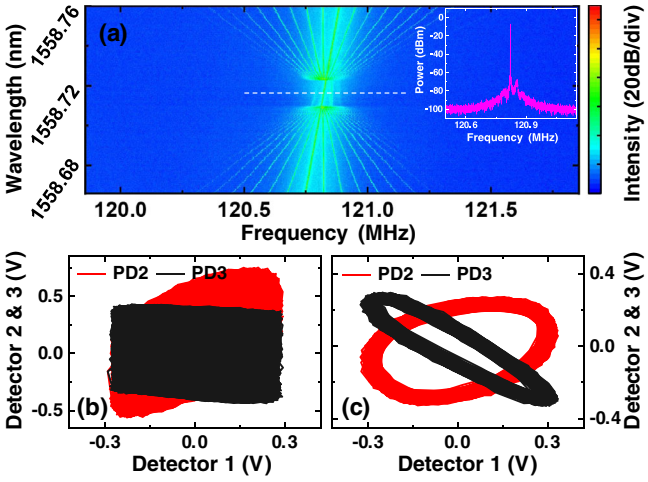

FIG. 4. (a) The optical field modulated by the microsphere and the microdisk with a 5-km-long single-mode fiber link, showing the dynamic process of synchronization. Inset: the spectrum corresponding to the dot line in Fig. 4(a). The phase portraits of the optomechanical oscillations corresponding to (b) before and (c) after synchronization.

trajectory clearly demonstrates the synchronization of frequencies and phases between the two oscillations [Fig. 3(g)]. The slight deviation of the portrait from an ellipsoidal shape is due to the integer multiples of the mechanical frequency generated by the four-wave mixing between the pump and sideband. The trajectory can be made more pronounced by increasing the seeding signals from the first oscillator to further suppress the PE.

Long-distance synchronization.—In future applications of the optomechanical system networks, the synchronization of remote oscillators by all-optical fiber links is necessary. The main challenge is the loss of transmission in the long single-mode fiber. If the fiber is so long that the loss attenuates the amplitude of the sideband tone from the microsphere to a very weak value, PE in the second resonator cannot be sufficiently suppressed. Here, we demonstrate the all-optical and long-distance synchronization between two mechanical oscillators linked by a 5 km fiber.

In this experiment, the input power decreases from 39.7 to 13.8 mW after the 5 km fiber, corresponding to a loss of 4.6 dB. It is pointed out that the higher optical power decreases observably after longer fibers due to the strong nonlinear effect in the fiber. Figure 4(a) shows the dynamic evolution of the PSD detected by PD2 as the pump laser scans around 1558.7 nm. With reduced pump detuning, the system evolves from the nonsynchronization state to the synchronization state, and finally back to the nonsynchronization state. The phase relations between the two resonators detected by PD1, PD2, and PD3 are presented in Figs. 4(b) and 4(c), corresponding to the nonsynchronization and synchronization phenomenon, respectively. The advantage of the all-optical method is that the pump and sideband go through the same fiber channel, thus the synchronization is robust against fluctuations of the fiber. For synchronization in longer distances, even though the loss of fibers limits the lower-power transfer efficiencies, the synchronization can be also realized by amplifying the sideband using gain components, such as gain fibers and optical parametric amplifiers.

Discussion.—In this Letter, we demonstrate the all-optical long-distance synchronization between the mechanical oscillators in a microsphere and a microdisk. By utilizing the thermal-optic and spring effects, we simultaneously tune the frequencies of the optical modes and mechanical modes in both resonators to match each other. Inside the injection locking range, we realize the synchronization between the microsphere and the microdisk over a 5-km-long fiber with only one drive laser. The phase locking is characterized by the power spectral density of the output field and the trajectory in the phase space. The long-distance and all-optical synchronization demonstrated in our experiment promises the construction of complex synchronization optomechanical systems networks using the current fiber network [20], which might find applications in optical communications and clock synchronization.

The work was supported by the National Key R&D Program of China (Grant No. 2020YFB2205801), the National Natural Science Foundation of China (Grants No. 11934012, No. 11874342, No. 61805229, and No. 92050109), USTC Research Funds of the Double First-Class Initiative (YD2470002002), and the Fundamental Research Funds for the Central Universities. C.-H. D. was supported the State Key Laboratory of Advanced Optical Communication Systems and Networks, Shanghai Jiao Tong University, China. This work was partially carried out at the USTC Center for Micro and Nanoscale Research and Fabrication.

*J. L., Z.-H. Z., and S. W. contributed equally to this work.
†lmwin@ustc.edu.cn
‡chunhua@ustc.edu.cn

[1] J.-D. Deschenes, L. C. Sinclair, F. R. Giorgetta, W. C. Swann, E. Baumann, H. Bergeron, M. Cermak, I. Coddington, and N. R. Newbury, Synchronization of Distant Optical Clocks at the Femtosecond Level, Phys. Rev. X **6**, 021016 (2016).

[2] S. Bregni, *Synchronization of Digital Telecommunications Networks* (Wiley, New York, 2002).

[3] K. Stephan, Inter-injection-locked oscillators for power combining and phased arrays, IEEE Trans. Microwave Theory Tech. **34**, 1017 (1986).

[4] A. F. Taylor, M. R. Tinsley, F. Wang, Z. Y. Huang, and K. Showalter, Dynamical quorum sensing and synchronization in large populations of chemical oscillators, Science **323**, 614 (2009).

[5] J. K. Jang, A. Klenner, X. Ji, Y. Okawachi, M. Lipson, and A. L. Gaeta, Synchronization of coupled optical microresonators, Nat. Photonics **12**, 688 (2018).

[6] X. Mao, Y. Sun, L. Wang, Y. Guo, Z. Gao, Y. Wang, S. Li, L. Yan, and A. Wang, Instability of optical phase synchronization between chaotic semiconductor lasers, Opt. Lett. **46**, 2824 (2021).
[7] M. H. Matheny, M. Grau, L. G. Villanueva, R. B. Karabalin, M. C. Cross, and M. L. Roukes, Phase Synchronization of Two Anharmonic Nanomechanical Oscillators, Phys. Rev. Lett. **112**, 014101 (2014).
[8] S.-B. Shim, M. Imboden, and P. Mohanty, Synchronized oscillation in coupled nanomechanical oscillators, Science **316**, 95 (2007).
[9] L. Ying, Y.-C. Lai, and C. Grebogi, Quantum manifestation of a synchronization transition in optomechanical systems, Phys. Rev. A **90**, 053810 (2014).
[10] W. Li, C. Li, and H. Song, Criterion of quantum synchronization and controllable quantum synchronization based on an optomechanical system, J. Phys. B **48**, 035503 (2015).
[11] K. Shlomi, D. Yuvaraj, I. Baskin, O. Suchoi, R. Winik, and E. Buks, Synchronization in an optomechanical cavity, Phys. Rev. E **91**, 032910 (2015).
[12] N. Yang, A. Miranowicz, Y.-C. Liu, K. Xia, and F. Nori, Chaotic synchronization of two optical cavity modes in optomechanical systems, Sci. Rep. **9**, 15874 (2019).
[13] D. Xu, Z.-Z. Han, Y.-K. Lu, Q. Gong, C.-W. Qiu, G. Chen, and Y.-F. Xiao, Synchronization and temporal nonreciprocity of optical microresonators via spontaneous symmetry breaking, Adv. Opt. Photonics **1**, 046002 (2019).
[14] C.-L. Zhu, Y.-L. Liu, L. Yang, Y.-X. Liu, and J. Zhang, Synchronization in PT-symmetric optomechanical resonators, Photonics Res. **9**, 2152 (2021).
[15] M. Aspelmeyer, T. J. Kippenberg, and F. Marquardt, Cavity optomechanics, Rev. Mod. Phys. **86**, 1391 (2014).
[16] C.-H. Dong, Y.-D. Wang, and H.-L. Wang, Optomechanical interfaces for hybrid quantum networks, Natl. Sci. Rev. **2**, 510 (2015).
[17] E. Verhagen and S. Deléglise, S. Weis, A. Schliesser, and T. J. Kippenberg, Quantum-coherent coupling of a mechanical oscillator to an optical cavity mode, Nature (London) **482**, 63 (2012).
[18] M. Eichenfield, J. Chan, R. M. Camacho, Kerry J. Vahala, and Oskar Painter, Optomechanical crystals, Nature (London) **462**, 78 (2009).
[19] Z. Fang, S. Haque, S. Farajollahi, H. Luo, J. Lin, R. Wu, J. Zhang, Z. Wang, M. Wang, Y. Cheng, and T. Lu, Polygon Coherent Modes in a Weakly Perturbed Whispering Gallery Microresonator for Efficient Second Harmonic, Optomechanical, and Frequency Comb Generations, Phys. Rev. Lett. **125**, 173901 (2020).
[20] Z. Shen, Z.-H. Zhou, C.-L. Zou, F.-W. Sun, G.-P. Guo, C.-H. Dong, and G.-C. Guo, Observation of high-Q optomechanical modes in the mounted silica microspheres, Photonics Res. **3**, 243 (2015).
[21] T. Li, T. Bao, Y. Zhang, C. Zou, X. Zou, and C. Guo, Long-distance synchronization of unidirectionally cascaded optomechanical systems, Opt. Express **24**, 12336 (2016).
[22] G. Heinrich, M. Ludwig, J. Qian, B. Kubala, and F. Marquardt, Collective Dynamics in Optomechanical Arrays, Phys. Rev. Lett. **107**, 043603 (2011).
[23] M. F. Colombano, G. Arregui, N. E. Capuj, A. Pitanti, J. Maire, A. Griol, B. Garrido, A. Martinez, C. M. Sotomayor-Torres, and D. Navarro-Urrios, Synchronization of Optomechanical Nanobeams by Mechanical Interaction, Phys. Rev. Lett. **123**, 017402 (2019).
[24] E. Gil-Santos, M. Labousse, C. Baker, A. Goetschy, W. Hease, C. Gomez, A. Lemaître, G. Leo, C. Ciuti, and I. Favero, Light-Mediated Cascaded Locking of Multiple Nano-Optomechanical Oscillators, Phys. Rev. Lett. **118**, 063605 (2017).
[25] M. Zhang, S. Shah, J. Cardenas, and M. Lipson, Synchronization and Phase Noise Reduction in Micromechanical Oscillator Arrays Coupled through Light, Phys. Rev. Lett. **115**, 163902 (2015).
[26] I. Bargatin, E. B. Myers, J. S. Aldridge, C. Marcoux, P. Brianceau, L. Duraffourg, E. Colinet, S. Hentz, P. Andreucci, and M. L. Roukes, Large-scale integration of nanoelectromechanical systems for gas sensing applications, Nano Lett. **12**, 1269 (2012).
[27] M. H. Matheny, M. Grau, L. G. Villanueva, R. B. Karabalin, M. C. Cross, and M. L. Roukes, Phase Synchronization of Two Anharmonic Nanomechanical Oscillators, Phys. Rev. Lett. **112**, 014101 (2014).
[28] M. Bagheri, M. Poot, L. Fan, F. Marquardt, and H. X. Tang, Photonic Cavity Synchronization of Nanomechanical Oscillators, Phys. Rev. Lett. **111**, 213902 (2013).
[29] M. Zhang, G. S. Wiederhecker, S. Manipatruni, A. Barnard, P. McEuen, and M. Lipson, Synchronization of Micromechanical Oscillators Using Light, Phys. Rev. Lett. **109**, 233906 (2012).
[30] S. Y. Shah, M. Zhang, R. Rand, and M. Lipson, Master-Slave Locking of Optomechanical Oscillators over a Long Distance, Phys. Rev. Lett. **114**, 113602 (2015).
[31] R. Leijssen, G. R. La Gala, L. Freisem, J. T. Muhonen, and E. Verhagen, Nonlinear cavity optomechanics with nanomechanical thermal fluctuations, Nat. Commun. **8**, ncomms16024 (2017).
[32] L. Qiu, I. Shomroni, P. Seidler, and T. J. Kippenberg, Laser Cooling of a Nanomechanical Oscillator to Its Zero-Point Energy, Phys. Rev. Lett. **124**, 173601 (2020).
[33] See Supplemental Material at http://link.aps.org/supplemental/10.1103/PhysRevLett.129.063605 for details.
[34] S. Wan, R. Niu, Z.-Y. Wang, J.-L. Peng, M. Li, J. Li, G.-C. Guo, C.-L. Zou, and C.-H. Dong, Frequency stabilization and tuning of breathing soliton in Si_3N_4 microresonators, Photonics Res. **8**, 1342 (2020).
[35] Z.-H. Zhou, C.-L. Zou, Y. Chen, Z. Shen, G.-C. Guo, and C.-H. Dong, Broadband tuning of the optical and mechanical modes in hollow bottle-like microresonators, Opt. Express **25**, 4046 (2017).
[36] X.-X. Hu, J.-Q. Wang, Y.-H. Yang, J. B. Surya, Y.-L. Zhang, X.-B. Xu, M. Li, C.-H. Dong, G.-C. Guo, H. X. Tang, and C.-L. Zou, All-optical thermal control for second-harmonic generation in an integrated microcavity, Opt. Express **28**, 11144 (2020).